

NASA/CR—2000-210055



Thermophysical Properties of GRCop-84

David L. Ellis
Case Western Reserve University, Cleveland, Ohio

Dennis J. Keller
RealWorld Quality Systems, Inc., Cleveland, Ohio

June 2000

The NASA STI Program Office . . . in Profile

Since its founding, NASA has been dedicated to the advancement of aeronautics and space science. The NASA Scientific and Technical Information (STI) Program Office plays a key part in helping NASA maintain this important role.

The NASA STI Program Office is operated by Langley Research Center, the Lead Center for NASA's scientific and technical information. The NASA STI Program Office provides access to the NASA STI Database, the largest collection of aeronautical and space science STI in the world. The Program Office is also NASA's institutional mechanism for disseminating the results of its research and development activities. These results are published by NASA in the NASA STI Report Series, which includes the following report types:

- **TECHNICAL PUBLICATION.** Reports of completed research or a major significant phase of research that present the results of NASA programs and include extensive data or theoretical analysis. Includes compilations of significant scientific and technical data and information deemed to be of continuing reference value. NASA's counterpart of peer-reviewed formal professional papers but has less stringent limitations on manuscript length and extent of graphic presentations.
- **TECHNICAL MEMORANDUM.** Scientific and technical findings that are preliminary or of specialized interest, e.g., quick release reports, working papers, and bibliographies that contain minimal annotation. Does not contain extensive analysis.
- **CONTRACTOR REPORT.** Scientific and technical findings by NASA-sponsored contractors and grantees.

- **CONFERENCE PUBLICATION.** Collected papers from scientific and technical conferences, symposia, seminars, or other meetings sponsored or cosponsored by NASA.
- **SPECIAL PUBLICATION.** Scientific, technical, or historical information from NASA programs, projects, and missions, often concerned with subjects having substantial public interest.
- **TECHNICAL TRANSLATION.** English-language translations of foreign scientific and technical material pertinent to NASA's mission.

Specialized services that complement the STI Program Office's diverse offerings include creating custom thesauri, building customized data bases, organizing and publishing research results . . . even providing videos.

For more information about the NASA STI Program Office, see the following:

- Access the NASA STI Program Home Page at <http://www.sti.nasa.gov>
- E-mail your question via the Internet to help@sti.nasa.gov
- Fax your question to the NASA Access Help Desk at (301) 621-0134
- Telephone the NASA Access Help Desk at (301) 621-0390
- Write to:
NASA Access Help Desk
NASA Center for Aerospace Information
7121 Standard Drive
Hanover, MD 21076

NASA/CR—2000-210055



Thermophysical Properties of GRCop-84

David L. Ellis
Case Western Reserve University, Cleveland, Ohio

Dennis J. Keller
RealWorld Quality Systems, Inc., Cleveland, Ohio

Prepared under Contract NAS3-463

National Aeronautics and
Space Administration

Glenn Research Center

June 2000

Acknowledgments

The authors would like to thank Raymond Taylor and the staff at TPRL, Inc. for conducting much of the thermophysical testing, answering questions regarding the testing and providing insight into the results.

The authors would also like to thank Patrick M. Martin of ORNL for conducting the low temperature electrical resistivity measurements.

Trade names or manufacturers' names are used in this report for identification only. This usage does not constitute an official endorsement, either expressed or implied, by the National Aeronautics and Space Administration.

Available from

NASA Center for Aerospace Information
7121 Standard Drive
Hanover, MD 21076
Price Code: A03

National Technical Information Service
5285 Port Royal Road
Springfield, VA 22100
Price Code: A03

Thermophysical Properties Of GRCop-84

David L. Ellis
Case Western Reserve University
Cleveland, OH 44106-7204

Dennis J. Keller
RealWorld Quality Systems, Inc.
Cleveland, OH 44116

Abstract

The thermophysical properties and electrical resistivity of GRCop-84 (Cu - 8 at.% Cr-4 at.% Nb) were measured from cryogenic temperatures to near its melting point. The data were analyzed using weighted regression to determine the properties as a function of temperature and assign appropriate confidence intervals.

The results showed that the thermal expansion of GRCop-84 was significantly lower than NARloy-Z (Cu-3 wt.% Ag-0.5 wt.% Zr), the currently used thrust cell liner material. The lower thermal expansion is expected to translate into lower thermally induced stresses and increases in thrust cell liner lives between 2X and 41X over NARloy-Z. The somewhat lower thermal conductivity of GRCop-84 can be offset by redesigning the liners to utilize its much greater mechanical properties. Optimized designs are not expected to suffer from the lower thermal conductivity. Electrical resistivity data, while not central to the primary application, show that GRCop-84 has potential for applications where a combination of good electrical conductivity and strength is required.

Introduction

New ternary Cu-Cr-Nb alloys are under consideration for use in several high heat flux, high temperature applications such as combustion chamber liners for regeneratively cooled rocket engines. One alloy, GRCop-84 (Cu - 8 at.% Cr - 4 at.% Nb) has been selected for further development in the Reusable Launch Vehicle (RLV) program. As part of the design of the engines, it is necessary to determine the mechanical and thermophysical properties of GRCop-84 over the potential operating conditions. This portion of the effort experimentally measured the thermal conductivity and thermal expansion of GRCop-84 from cryogenic temperatures to near the melting point of the alloy and assigned confidence intervals on those measurements.

NARloy-Z (Cu-3 wt.% Ag-0.5 wt.% Zr) is currently used for the space shuttle main engine (SSME). NARloy-Z possesses very high thermal conductivity, but suffers from lower than desired elevated temperature mechanical properties. GRCop-84 has shown considerably better mechanical properties (1 - 3) but a lower thermal conductivity. As part of the trade studies required for the alloy selections and design of the engines, the benefits of increased mechanical and other properties will be weighed against the lower thermal conductivity. NARloy-Z is also 5% denser than GRCop-84. For the RLV program where the design could call for hundreds of small thrust cells, the lower density can translate into lower engine weight, increased thrust-to-weight ratio and larger payloads.

Experimental Procedure

Alloy Production

Five separate powder production runs or lots of GRCop-84 were made at Crucible Research in Pittsburgh, PA. Each powder lot was kept separate during production and consolidation so they represent true statistical repeats. Each powder lot was canned in three 15.2 cm (6 inch) diameter mild steel extrusion cans by Crucible Research and delivered to CSM Industries in Coldwater, MI for extrusion. Each can was extruded using a reduction in area ratio of 29.5, which resulted in a total of 15 extruded bars with an average diameter of 2.8 cm (1.1 inches) and an average length of 3.96 m (13 feet). One sample was taken from each extrusion for each type of testing.

Thermophysical Testing

Because of the need for specialized equipment, most of the thermophysical testing was conducted at TPRL Inc. in West Lafayette, IN. Elevated temperature thermal expansion testing was conducted at the NASA Glenn Research Center in Cleveland, OH, to complete the database.

Thermal Conductivity

Thermal conductivity was measured and calculated by various methods from 30 K (-405°F) to 1173 K (1652°F).

For testing at room temperature and above, the laser flash technique was employed. This technique requires the measurement of the room temperature bulk density (ρ_{RT}), the specific heat (c_p) and the thermal diffusivity (α). The room temperature bulk density was measured using a Micromeritics AccuPyc 1330 pycnometer and an Ainsworth AA-160 digital balance. The specific heat was measured using a Perkin-Elmers Model DSC-2 Differential Scanning Calorimeter (DSC) from room temperature to 573 K (572°F). Between 573 K and 1173 K and below room temperature, a Netzsch Model 404 DSC was used to measure the specific heat. Both DSCs used a sapphire standard. Thermal diffusivity was determined by heating a specimen to the desired temperature and subjecting the front face of the sample to a short laser burst. By monitoring the small rise in temperature of the back side with time and knowing the thickness of the sample, the thermal diffusivity can be calculated. The thermal conductivity (λ) at temperature T was then calculated using (4)

$$\lambda(T) = \alpha(T) c_p(T) \rho_{RT} \quad [1]$$

For thermal conductivity testing from below room temperature to about 473 K, the Kohlrausch method (5) was used. The sample was resistively heated by passing a direct current through the sample while the ends were kept at a constant temperature. This establishes a thermal gradient along the length of the sample which is measured by thermocouples placed at the center of the specimen and 1.0 cm (0.39 inches) to both sides of the center. In addition, the two outer thermocouples are also used as voltage probes to measure the voltage drop across the specimen. To minimize radial heat loss, the sample is surrounded by a heater that is maintained at the temperature of the center thermocouple. When steady state is achieved, the axial temperature distribution is a parabola.

The product of the thermal conductivity and electrical resistivity at any temperature can be calculated from

$$\lambda(T_2)\rho(T_2) = \frac{(V_3 - V_1)^2}{4[2T_2 - (T_1 + T_3)]} \quad [2]$$

where $V_3 - V_1$ is the voltage drop measured by the outer thermocouples, T_2 is the center temperature, and T_1 and T_3 are the outer temperatures. The resistivity of the specimens can be calculated knowing the cross-sectional area (A) and the current passing through the specimen (I) using the equation

$$\rho = \frac{(V_3 - V_1) A}{I l} \quad [3]$$

where l is equal to the 2 cm distance between the thermocouples. After achieving steady state, all values needed are measured and the current through the sample increased to increase the temperature for the next measurement.

Low Temperature Electrical Resistivity

TPRL Inc. sent one specimen from powder lot 3C to the Superconductor Group at Oak Ridge National Laboratory (ORNL) for low temperature electrical resistivity testing. The resistivity of the sample was determined using the four point resistance method. A current between 1 and 40 mA was supplied by an HP 3245 Universal V/I source at 27 Hz. The voltage drop across the sample was read by a Par 5209 Lock-in Amplifier. To measure the temperature, a diode was placed on the sample between the voltage probes. A Lake Shore 330 Temperature Controller was used to record the temperature. The sample was cooled in vacuum using a CVI model CGR 409 UHV closed cycle refrigerator. After cooling to 30 K or lower, data were recorded during the warming of the sample back to room temperature.

Thermal Expansion

Push rod dilatometers were used to measure the thermal expansion of the specimens. The sample is placed in a holder with a rod pushing against one end of the specimen. As the specimen is heated or cooled, the change in length of the specimen is measured by a linear variable differential transformer (LVDT) attached to the opposite end of the push rod. Software compensates for the thermal expansion of the holder and push rod. A thermocouple in intimate contact with the specimen is used to record the temperature. Cryogenic thermal expansion testing was done at TPRL Inc. Elevated temperature testing was done at NASA GRC using an Orton model 1600C dilatometer. To protect the specimens from oxidation at elevated temperatures, the holder was enclosed in a furnace tube and He flowed through the assembly. The results were recorded at 1 K (1.8°F) intervals for the elevated temperature tests and at approximately 10 K (18°F) intervals for the cryogenic tests.

Results

Alloy Chemistries

The chemistries of the extruded bars are listed in Table 1. For brevity, the chemistries from the three extrusions in each powder lot are averaged and the standard deviations presented to show variability in the values. In general, the values were almost identical for each extrusion within a powder lot. The only major change in chemistry from the raw powder was a slight increase in oxygen content that occurred during processing.

The chemistries show a small but detectable amount of Fe present in the alloys. This has been traced to the Cr melt stock used to make the alloys. Although the Cr is reported to be 99.99% purity, it actually had significant Fe present. The Fe made it through the melting and subsequent processing to become a trace impurity in the alloy.

Table 1 - Chemistry Of Extruded GRCop-84

Powder Lot		Cr		Nb		Cr:Nb Ratio		Cr+Nb		Calculated Cr ₂ Nb vol.%	Fe ppm	O ppm
		wt.%	at.%	wt.%	at.%	wt.%	at.%	wt.%	at.%			
3A	Average	6.68	8.21	5.72	3.92	1.17	2.09	12.41	12.13	14.20	157	720
	σ	0.06	0.07	0.02	0.01	0.01	0.01	0.08	0.08	0.09	6	18
3B	Average	6.59	8.06	5.66	3.88	1.16	2.08	12.23	11.94	14.00	167	694
	σ	0.06	0.06	0.03	0.02	0.00	0.01	0.08	0.08	0.08	6	9
3C	Average	6.66	8.16	5.79	3.98	1.15	2.05	12.45	12.14	14.24	193	492
	σ	0.03	0.03	0.03	0.02	0.00	0.00	0.05	0.04	0.05	6	9
3D	Average	6.55	8.04	5.69	3.91	1.15	2.06	12.25	11.95	14.01	153	562
	σ	0.02	0.03	0.03	0.02	0.01	0.01	0.04	0.03	0.04	6	30
3E	Average	6.58	8.11	5.78	3.97	1.14	2.04	12.39	12.08	14.22	167	414
	σ	0.01	0.08	0.02	0.01	0.01	0.02	0.07	0.08	0.06	12	32

Statistical Analysis

The data generated allowed a statistical regression analysis to be conducted that resulted in fitted equations to the data. Even more important for design work, the data allowed for the calculation of confidence intervals on the data. For the statistical analysis, the work was divided into two complementary analyses; a series of one-way Analysis of Variances (ANOVAs) at each temperature of interest and a regression analysis on the data from all temperatures.

The one-way ANOVA at each temperature was used to determine if there were statistically significant powder lot-to-powder lot variances. Extrusion-to-extrusion variances, which included variation due to the testing process, were used as the lowest level error for testing significances of powder lot-to-powder lot variances. When powder lot-to-powder lot differences were observed, the analysis allowed for the ranking of the extrusions from lowest to highest value using a multiple comparisons of means procedure.

The ANOVA also permitted the analysis of the error structure. Such an analysis not only determined the magnitude of the overall variation (or errors), denoted S_{Total} , at each data point, but also determined if the S_{Total} were consistent (a homoscedastic error structure) or changing (a heteroscedastic error structure) across all temperatures. Each S_{Total} was a composite error estimate that included both powder lot-to-powder lot variation and extrusion-to-extrusion variation. The degrees of freedoms for the resultant S_{Total} estimates were calculated using a Satterthwaite's formula which employs a weighted harmonic average of the degrees of freedom of the two components; powder lot-to-powder lot and extrusion-to-extrusion. It was found that the error structure was indeed heteroscedastic (i.e. the S_{Total} were not consistent across all temperatures). This meant that a weighted regression analysis of the data would be necessary in the subsequent development of predictive models and confidence intervals. In all cases, the simplest equation that accurately fit the data and predicted the observed trends was used although a higher order equation could have been fit to the data.

Recall, however, that an estimate of the error structure, S_{Total} , was only available at each data point. This fact is sufficient for running a weighted regression, since such an analysis requires weights only at each data point. The weights typically used are $1/(S_{Total})^2$. However, for the construction of confidence intervals for future model predictions, estimates of the error structure at all temperatures are required. To get over this hurdle, a standard regression analysis was conducted on the error structure itself. The results were a simple model that predicted the error structure, S_{Total} , over the entire temperature range. These predicted S_{Total} were also used in determining the weights as $1/(S_{Total})^2$ in the weighted regression.

An approximate $(1 - \alpha)100\%$ confidence interval on future model predictions is given by the formula

$$Y_{CI}(T) = f(T) \pm t(1 - \alpha, \nu) S_{Y,X}(T) \quad [4]$$

where

- $Y_{CI}(T)$ = the approximate $(1 - \alpha)100\%$ confidence interval for a future model prediction for property Y at temperature T
 $f(T)$ = the resultant regression equation for prediction of the property Y from temperature T
 $t(1 - \alpha, \nu)$ = t value for a given confidence $(1 - \alpha)$ and degrees of freedom (ν)
 $S_{Y,X}(T)$ = the standard error of the regression which is typically estimated under the assumption of homoscedastic errors as

$$S_{Y,X} = \sqrt{\frac{\sum (Y_{Actual} - Y_{Predicted})^2}{N - P}} \quad [5]$$

where N = number of data points and P = number of parameters being estimated

The standard error of the regression, $S_{Y,X}$, is a measure of goodness of fit of the model to the data. It is made up of two components; pure error and lack-of-fit (LOF). The pure error component was already estimated in S_{Total} and was found to be heteroscedastic. Hence, $S_{Y,X}$ could not be estimated in the usual way, but had to be manufactured from S_{Total} and an estimate of the LOF component. The LOF component is typically a measurement of the deviation of the mean of the property Y repeats from the model predicted value or in equation form

$$S_{LOF} = \sqrt{\frac{\sum (Y_{Actual\ Mean} - Y_{Predicted})^2}{K - 1}} \quad [6]$$

where K is the number of means or the number of unique temperatures. Finally, an estimate of $S_{Y,X}$ that captured the heteroscedastic nature of the error structure was constructed using

$$S_{Y,X}(T) = \sqrt{S_{LOF}^2 + S_{Total}^2(T)} \quad [7]$$

Hence, the approximate $(1 - \alpha)100\%$ confidence intervals on future model predictions was calculated according to Equations 4 and 7.

Thermal Diffusivity

The results of the thermal diffusivity testing are shown in Figure 1. Eleven one-way ANOVAs were conducted to determine if there were statistically significant powder lot-to-powder lot differences. The statistical analysis did not reveal any significant differences. The error structure was analyzed, and it was found that the standard error of regression ($S_{Y,X}$) at any temperature within the range tested is given by the equation

$$S_{Y,X}(T) = \sqrt{S_{LOF}^2 + S_{Total}^2(T)} \quad [8]$$

$$= \sqrt{(2.392 \times 10^{-3})^2 + (6.654 \times 10^{-3} + 2.660 \times 10^{-6} T)^2}$$

Using the appropriate values of S_{Total} , a weighted regression was performed on the data. The thermal diffusivity (cm^2/s) as a function of temperature (K) is given by the equation

$$\alpha(T) = 0.8726 - 1.910 \times 10^{-4} T + 4.153 \times 10^{-7} T^2 - 3.588 \times 10^{-10} T^3 \quad [9]$$

For combustion chamber liners and other heat exchangers, the lower limit of thermal diffusivity is needed to design the parts. The data have an average of eleven degrees of freedom (ν), so the resulting t value for determining the lower confidence interval is 1.796. Using Equation 4 with only a lower confidence interval gives the equation for the lower 95% confidence interval as

$$\alpha_{Lower\ 95\%}(T) = \alpha(T) - t(0.95, 11) S_{Y,X}(T) \quad [10]$$

$$= 0.8726 - 1.910 \times 10^{-4} T + 4.153 \times 10^{-7} T^2 - 3.588 \times 10^{-10} T^3$$

$$- 1.796 \sqrt{(2.392 \times 10^{-3})^2 + (6.654 \times 10^{-3} + 2.660 \times 10^{-6} T)^2}$$

The value used of $t(1 - \alpha, 11) = 1.796$ can be changed to reflect any other confidence limit or modified to a two-sided value if upper and lower confidence intervals are desired.

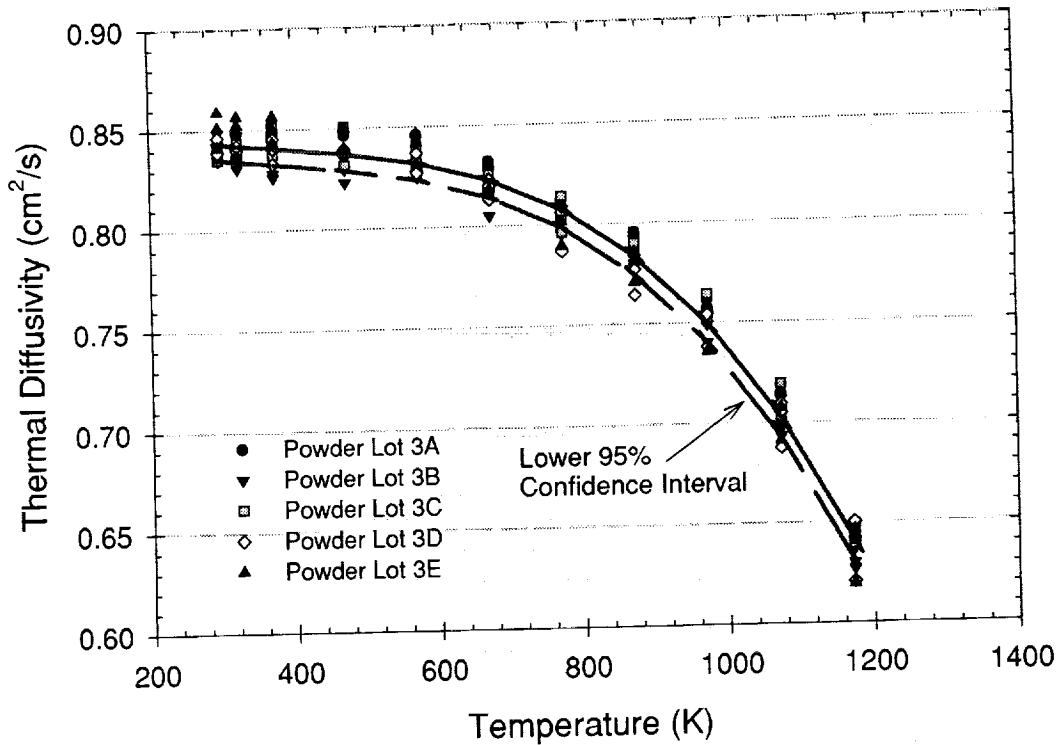


Figure 1 - Thermal Diffusivity Of GRCop-84

Specific Heat

The specific heat results are shown in Figure 2. The twenty-six one-way ANOVAs showed that in thirteen cases (296 K, 623 K to 1173 K) there were statistically significant powder lot-to-powder lot variances. In all thirteen cases, powder lot 3C had a significantly higher specific heat than powder lot 3D. In twelve of the cases, powder lot 3C also had a significantly higher specific heat than powder lot 3B, and in six cases powder lot 3C had a significantly higher specific heat than powder lot 3E. Visual examination of Figure 2 also indicates these relationships. The heat capacities of powder lot 3C are always higher than lots 3B and 3D in the plot.

As with the thermal diffusivity data, the value of S_{Total} at each temperature was calculated and the error structure analyzed. This time the values for S_{Total} could not be fit with a straight line. Instead, a cubic equation was needed. The resulting standard error of regression is given by the equation

$$S_{j,i}(T) = \sqrt{(3.827 \times 10^{-3})^2 + (2.108 \times 10^{-2} - 9.165 \times 10^{-5}T + 1.433 \times 10^{-7}T^2 - 6.392 \times 10^{-11}T^3)^2} \quad [11]$$

Using the appropriate values of S_{Total} , a weighted regression was done on the data. The specific heat (J/gK) as a function of temperature (K) is given by the equation

$$c_p(T) = 0.2539 + 6.563 \times 10^{-4}T - 8.903 \times 10^{-7}T^2 + 4.292 \times 10^{-10}T^3 \quad [12]$$

For the planned application, the lower confidence interval would be used for designing the liner. The data have an average of eight degrees of freedom, so the resulting t value for determining the lower confidence interval is 1.860. The lower 95% confidence interval for the specific heat is given by the equation

$$c_{p,Lower,95\%}(T) = \frac{0.2539 + 6.563 \times 10^{-4}T - 8.903 \times 10^{-7}T^2 + 4.292 \times 10^{-10}T^3}{1.860 \sqrt{(3.827 \times 10^{-3})^2 + (2.108 \times 10^{-2} - 9.165 \times 10^{-5}T + 1.433 \times 10^{-7}T^2 - 6.392 \times 10^{-11}T^3)^2}} \quad [13]$$

As with the thermal diffusivity, the value of $t(1-\alpha,8) = 1.860$ can be changed to reflect different confidence intervals or two sided confidence intervals.

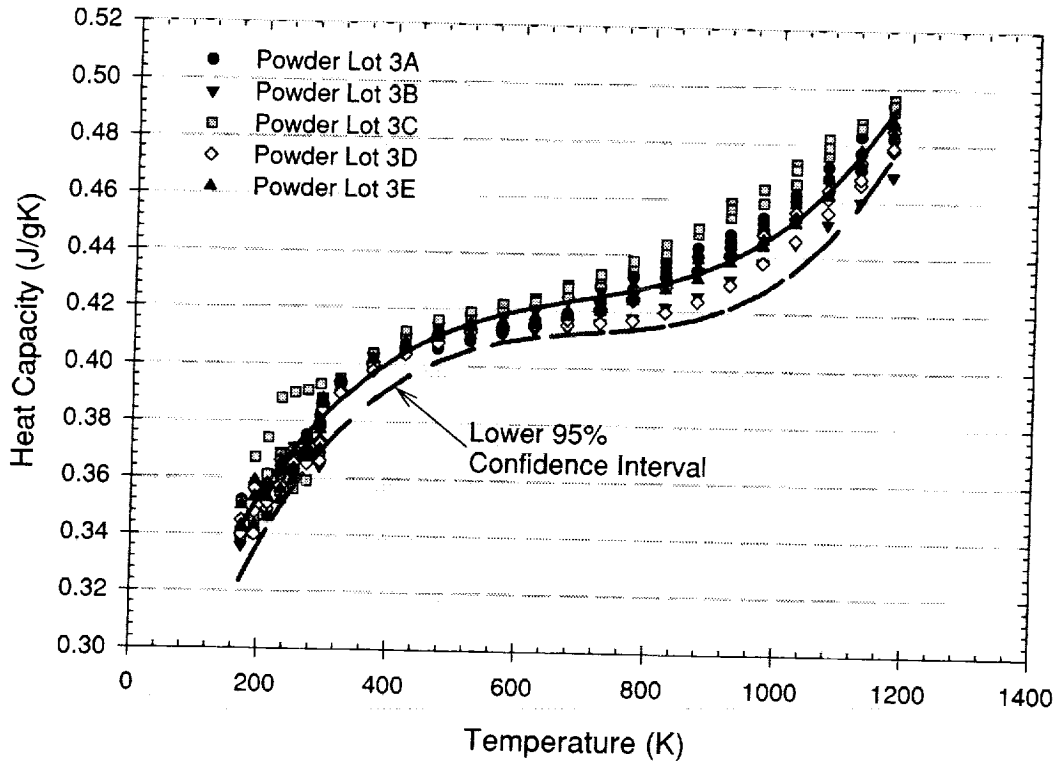


Figure 2 - Specific Heat of GRCop-84

Thermal Conductivity

The combined thermal conductivity test results are presented in Figure 3. For the statistical analysis of powder lot to powder lot variability, it was necessary to limit the data analyzed to those generated from room temperature to 1173 K using the laser flash technique. Eleven one-way ANOVAs were conducted. In five cases (373 K, 673 K, 873 K, 973 K and 1073 K), statistically significant powder lot-to-powder lot variances were observed. As with the heat capacities, a multiple comparison procedure was used to rank the thermal conductivities of the powder lots from lowest to highest. In all five cases, powder lot 3B had significantly lower thermal conductivity than powder lot 3C.

Again, the error structure was analyzed. In this case, the values of S_{Total} could be described by a straight line with an intercept of zero. The values for $S_{Y,X}$ are given by the equation

$$S_{Y,X}(T) = \sqrt{(2.405)^2 + (7.934 \times 10^{-3} T)^2} \quad [14]$$

A weighted regression using the appropriate values of $S_{Y,X}$ yielded the equation relating thermal conductivity (W/mK) to temperature (K) over the temperature range of 296 K to 1173 K as being

$$\lambda(T)_{296-1173} = 243.8 + 0.1792 T - 1.325 \times 10^{-4} T^2 \quad [15]$$

The data have an average of eight degrees of freedom, so the resulting t value for determining the lower confidence interval is 1.860. Since the lower limit of thermal conductivity is needed for thrust cell liner applications, the lower confidence interval was selected again. The resulting equation for the lower 95% confidence interval is

$$\lambda(T)_{296-1173, \text{Lower } 95\%} = 243.8 + 0.1792 T - 1.325 \times 10^{-4} T^2 - 1.860 \sqrt{(2.405)^2 + (7.934 \times 10^{-3} T)^2} \quad [16]$$

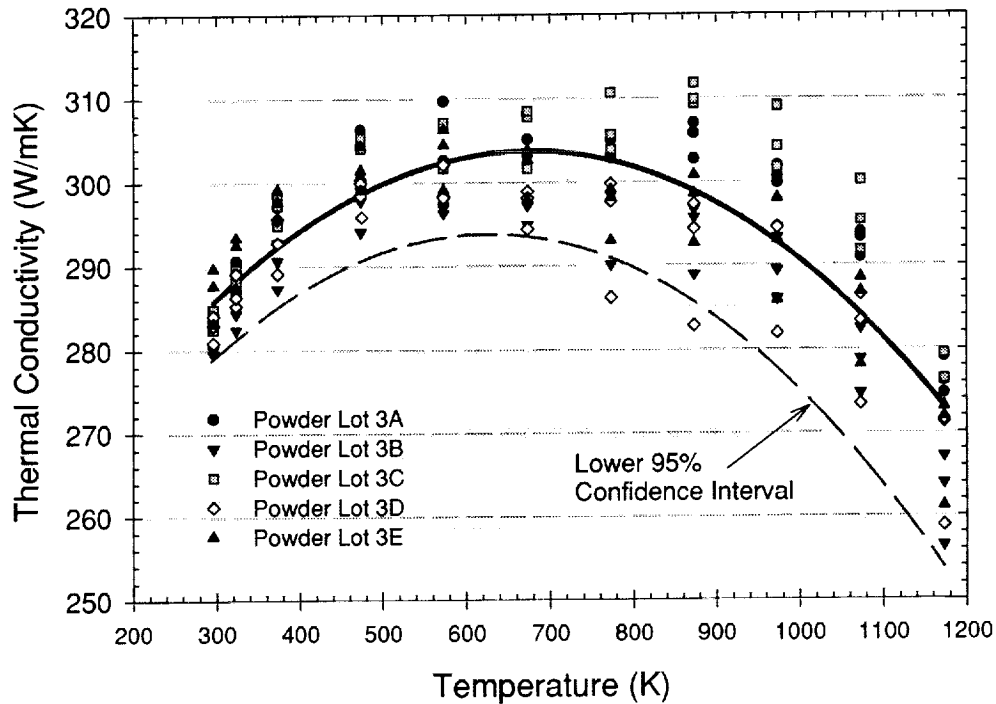


Figure 3 - Elevated Temperature Thermal Conductivity of GRCop-84

It should be remembered that Equations 14-16 apply only over the temperature range of 296 K to 1173 K. To extend the analysis to lower temperatures requires adding the data from the Kohlrausch tests.

The data from the Kohlrausch technique did not fall at regular temperature intervals, so it does not lend itself easily to statistical analysis. However, if the simplifying assumption is made that the errors are homoscedastic rather than heteroscedastic, an unweighted regression can be done on all data and a lower 95% confidence limit assigned to the entire temperature range tested. The resulting equation relating the thermal conductivity (W/mK) to temperature (K) is

$$\lambda(T)_{All} = 6893 - 3466 \ln(T) + 599.5 [\ln(T)]^2 - 34.18 [\ln(T)]^3 \quad [17]$$

Figure 4 shows all thermal conductivity data and the results of the unweighted regression. The value of $S_{Y,X}$ for all the data was 6.633. Using the average eight degrees of freedom again, the t value for the lower 95% confidence interval was determined to be 1.860. The approximate lower 95% confidence interval shown in Figure 4 is given by the equation

$$\lambda(T)_{All, Lower 95\%} = 6893 - 3466 \ln(T) + 599.5 [\ln(T)]^2 - 34.18 [\ln(T)]^3 - 1.860 \times 6.633 \quad [18]$$

As with the other data, the value of $t(1-\alpha,8) = 1.860$ can be changed to reflect different confidence intervals or two sided confidence intervals.

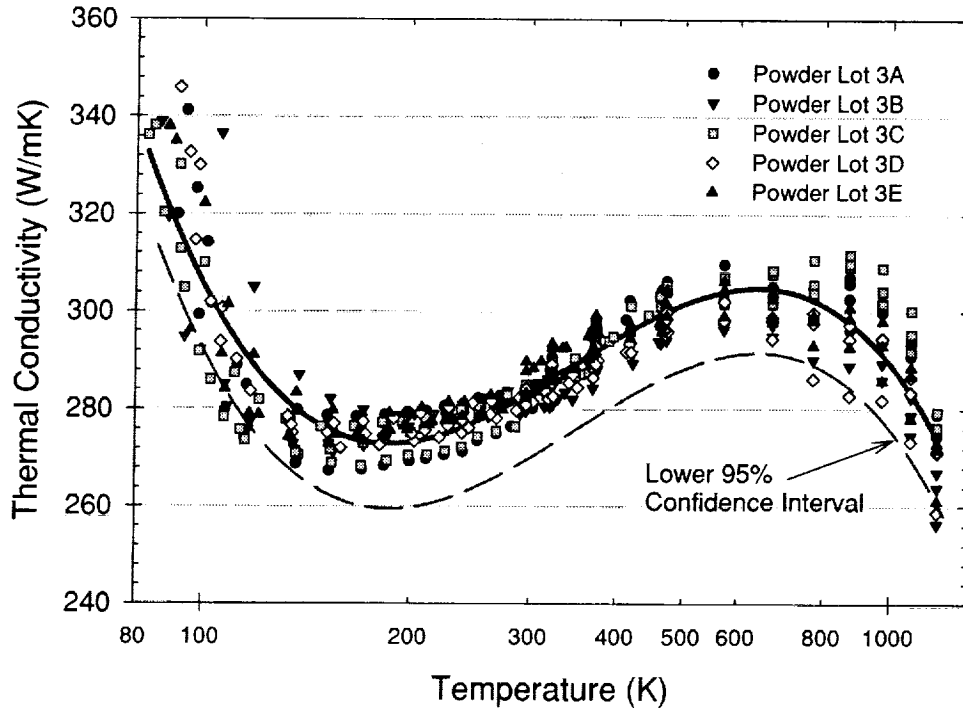


Figure 4 - Thermal Conductivity of GRCop-84 Using Unweighted Regression

Electrical Resistivity and Lorenz Number

The electrical resistivities measured during the Kohlrausch thermal conductivity testing are presented in Figure 5. As is readily apparent, there are no detectable powder lot-to-powder lot variations. A simple unweighted linear regression gives the dependency of electrical resistivity on temperature as

$$\rho(T) = -7.170 \times 10^{-2} + 8.570 \times 10^{-3} T \quad [19]$$

Since both the thermal conductivity and the electrical resistivity are measured simultaneously, the Lorenz number used in the Wiedmann-Franz Law (6) can be easily calculated. The values obtained as a function of temperature are presented in Figure 6. For reference, the ideal value of $2.45 \times 10^{-8} \text{ W}\Omega/\text{K}^2$, and the room temperature value for pure copper of $2.23 \times 10^{-8} \text{ W}\Omega/\text{K}^2$ are also presented.

Figure 7 shows the results of the ORNL low temperature electrical resistivity testing. Unlike the other tests, data were taken using only one sample from powder lot 3C. The data were examined for a T^5 dependency in accordance with the low temperature Bloch Equation (7). The resistivity was proportional to T^5 between 29 K and 40 K. Above 60 K the data and the T^5 curve were increasingly divergent. The best fit for the entire temperature range was obtained with the equation

$$\rho(T) = 0.2865 - 2.886 \times 10^{-3} T + 1.021 \times 10^{-4} T^2 - 2.859 \times 10^{-7} T^3 \quad [20]$$

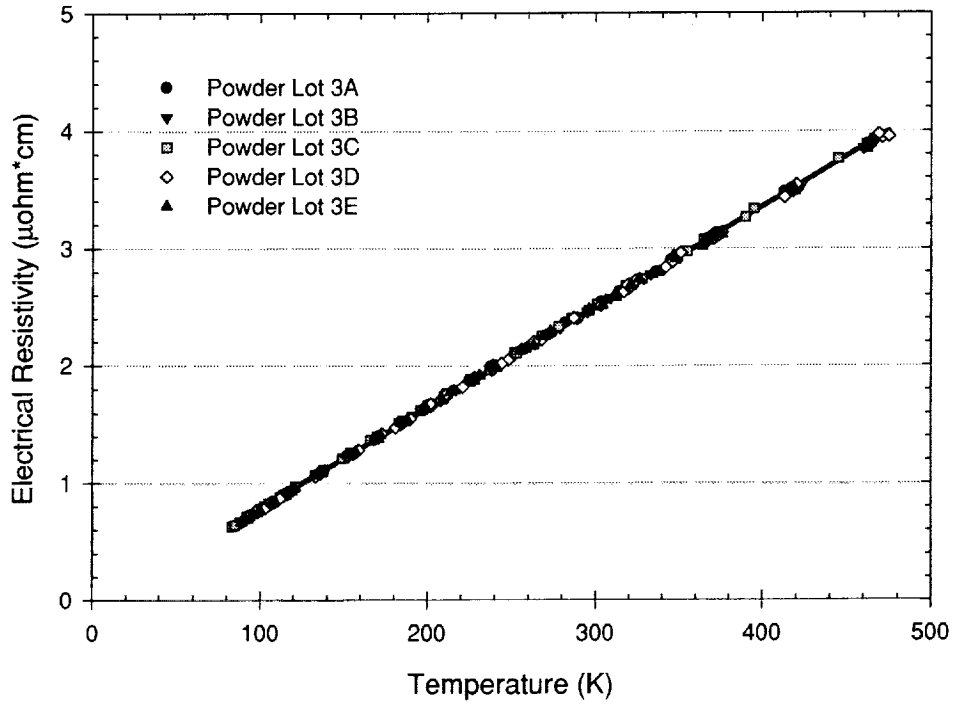


Figure 5 - Electrical Resistivity of GRCop-84

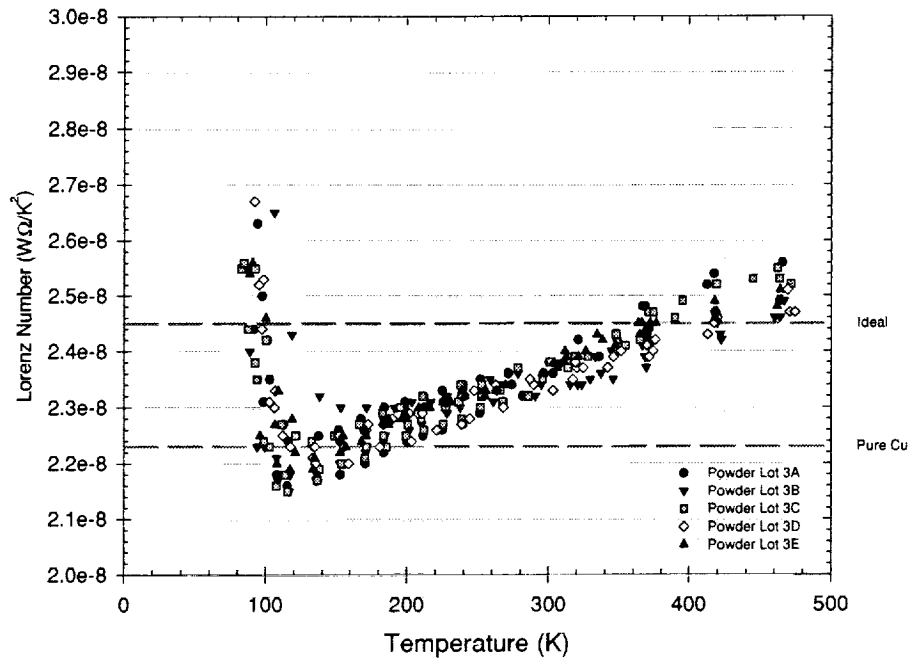


Figure 6 - Lorenz Number of GRCop-84

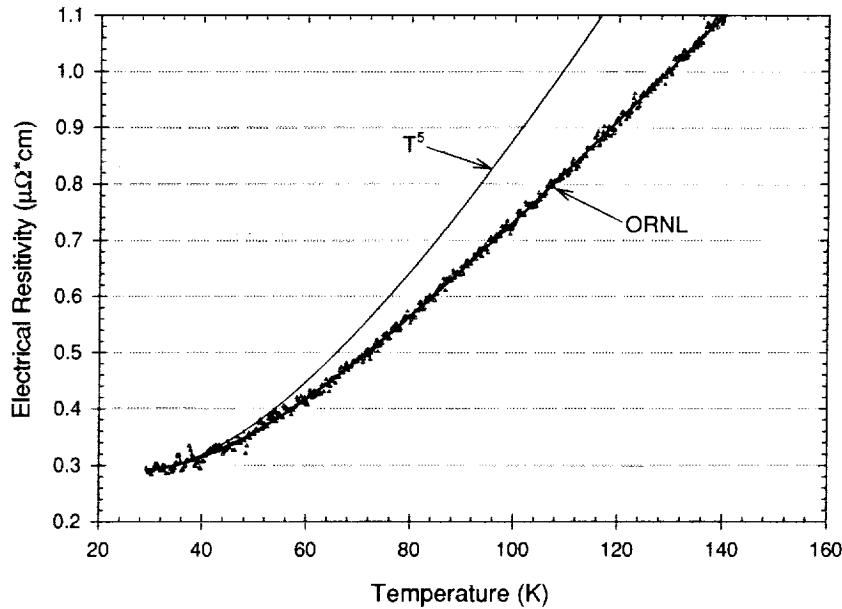


Figure 7 - GRCop-84 Low Temperature Electrical Resistivity (Powder Lot 3C)

Thermal Expansion

The results for the thermal expansion testing are shown in Figure 8. To allow statistical analysis of the data, it was necessary to reduce the data set by using a representative subset of the data. For the elevated temperature data, results at 299 K (79°F), 373 K (212°F) and every 100 K thereafter up to 1173 K (1652°F) were used. For the cryogenic data, the results at 293 K, 273 K (32°F), 173 K (-69°F) and 70 K (-333°F) were selected.

Fourteen one-way ANOVAs were conducted at each temperature to determine if there was a significant powder lot to powder lot variation. None was detected. As with the other results, the errors were determined to be heteroscedastic. This can be seen in Figure 8 as the spreading out of the curves as temperature increases. The error structure was analyzed, and the values of S_{Total} could be fit with a parabola. The values of $S_{Y,X}$ are given by the equation

$$S_{Y,X}(T) = \sqrt{(1.403 \times 10^{-2})^2 + (2.038 \times 10^{-5} T^2)} \quad [21]$$

A weighted regression was conducted on the thermal expansion data using the appropriate values of S_{Total} . The simplest equation that fits the data is a modified power law. The resulting equation relating thermal expansion (%) as a function of temperature (K) is

$$\alpha(T) = -0.3287 + 2.265 \times 10^{-4} T^{1.285} \quad [22]$$

The regression line in Figure 8 has been extrapolated to 1375 K to allow differentiation of it from the individual curves. Equation 22 is only valid to 1273 K, though.

Higher thermal expansions translate into higher thermally induced stresses and lower lives for combustion chamber liners, so the upper 95% confidence interval was selected. The data have an average of ten degrees of freedom, so the resulting t value for determining the upper limit is 1.812. The equation for the upper limit of thermal expansion is

$$\alpha(T)_{Upper\ 95\%} = (-0.3287 + 2.265 \times 10^{-4} T^{1.285}) + 1.812 \sqrt{(1.403 \times 10^{-2})^2 + (2.038 \times 10^{-5} T^2)} \quad [23]$$

The confidence interval is plotted in Figure 8 along with the data. Again, as with the other data, the value of $t(1-\alpha, 10) = 1.812$ can be changed to reflect different confidence intervals or two sided confidence intervals.

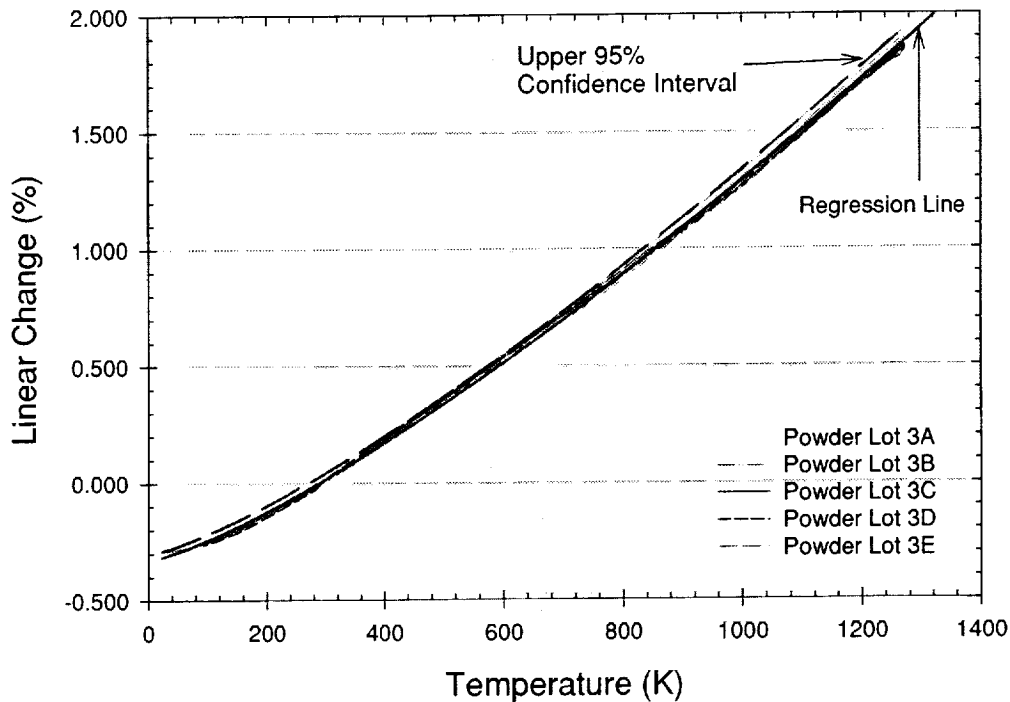


Figure 8 - Thermal Expansion of GRCop-84

Discussion

Statistical Analysis

It is important to remember that all statistical analyses are limited to the temperature and composition ranges tested. Extrapolation outside these ranges will result in rapidly increasing prediction errors. Most properties are covered from cryogenic temperatures to near the melting point, so temperature is a minor constraint. The composition of the alloy has been fixed, so the composition range tested is representative of future production runs.

The statistical analysis was driven by the need to have relatively simple, continuous equations to describe the properties as a function of temperature. Computer code used for finite element analysis and other design tools can then utilize the equations for determining thermal gradients, thermal expansions and related effects of the heat flux on the material. Because the material will be used in man-rated vehicles, it was also imperative to establish confidence intervals on the properties. The design of thrust cell liners utilizes either a lower or upper confidence interval since each property is unmistakably worse for the application in one direction only. For example, clearly only a decrease in thermal conductivity is bad since the liner temperature would increase, so only the lower confidence limit needs to be considered.

For each property, a two-stage statistical analysis of the data was conducted. In Stage 1, an error structure analysis was conducted. This analysis quantified two sources of error at each temperature; powder lot-to-powder lot (S_{PL}) and extrusion-to-extrusion (S_{EXT}) which also includes test error. These two sources are combined using the equation

$$S_{Total} = \sqrt{S_{PL}^2 + S_{EXT}^2} \quad [24]$$

to obtain an estimate of total variability in the "replicates" (S_{Total}) at each temperature. If the values of S_{Total} were consistent across all temperatures (i.e. homoscedastic), then an unweighted regression analysis could be conducted in Stage 2 for both fitting an equation to the data and more importantly for easily estimating $(1-\alpha)100\%$ confidence intervals on future predicted values.

The results of the Stage 1 analyses showed that in all cases the values of S_{Total} were not consistent (i.e. heteroscedastic) across the temperature region. This required that weighted regression be used in Stage 2 of the statistical analysis. For such an analysis, only weights at each temperature tested are needed. The weights employed were the typical $1/(S_{Total})^2$. However, for generating the estimated $(1-\alpha)100\%$ confidence intervals on future predicted values, an estimate of the error at all temperatures is required, not just at the temperatures for which there were data. This, therefore, required an additional step in the analysis sequence in which the error structure itself (S_{Total}) was modeled as a function of temperature. Then an estimated value for S_{Total} could be had for any

temperature. These predicted S_{Total} values were used in calculating the weights for the weighted regression. They were also used in calculating the estimated $(1-\alpha)100\%$ confidence intervals on future predicted values as shown in the Results section.

As mentioned before, the widths of the estimated $(1-\alpha)100\%$ confidence intervals on future predicted values are simply $t(1-\alpha, \nu)S_{Y,X}$. $S_{Y,X}$ is made up of two components; pure error and lack-of-fit (LOF). The pure error component, S_{Total} , was estimated in Stage 1 and was found to be heteroscedastic. Hence, $S_{Y,X}$ could not be estimated in the usual way (i.e. Equation 5), but had to be manufactured from S_{Total} and an estimate of the LOF component as shown in Equation 7. The LOF component measures how far off the model predictions are from the mean of property Y replicates. A "good" model, i.e., one without significant LOF, should have close agreement between the mean value of the response and the predicted value of the response. The LOF component was estimated using Equation 6. Lastly and specific to this work, a heteroscedastic standard error of the regression as a function of temperature, $S_{Y,X}(T)$, was manufactured from the estimated heteroscedastic pure error component $S_{\text{Total}}(T)$ and the estimated LOF component using Equation 7. This value of $S_{Y,X}(T)$ was then used to calculate the width of the estimated $(1-\alpha)100\%$ confidence intervals on future predicted values as just $t(1-\alpha, \nu)S_{Y,X}(T)$.

Notice that the t value is also important in setting the confidence interval. In this case, one-sided 95% confidence intervals were generated for all the properties. Changing the confidence level can be easily accomplished by substituting the t value for the same number of degrees of freedom (ν) but a different confidence level $(1-\alpha)$. However, it must be remembered that a simplifying assumption was made to use an integral average number of degrees of freedom rather than the degrees of freedom at each temperature. To determine the effects of the degrees of freedom on the t value, the worst case, specific heat, was examined. The lowest number of degrees of freedom from the Satterthwaite's formula was 5.3 at 1073 K. An average of eight degrees of freedom was used for the determination of the confidence interval. From a table of t values, the t value at a 95% confidence level would increase from 1.860 to 2.015 if five degrees of freedom are used. This represents a change of 8.3%. Therefore, the error term in Equation 9 would increase from 0.0180 J/gK to 0.0195 J/gK at 1073 K. On the scale of Figure 2, this represents lowering the confidence interval one minor division on the Y axis. It also represents less than 0.5% change in the value for the confidence interval. The results are similar for other temperatures where the degrees of freedom are less than eight. Based on this, the decision to use an average degrees of freedom was deemed to be justified.

Finally, it must be pointed out that because of the methods used and the simplifying assumptions, strictly speaking, the confidence intervals are estimates. However, because of the large number of data points generated during testing, simple comparison of the confidence intervals to the data can reveal if the estimates are valid. For a 95% confidence interval, if one hundred data points are plotted five should fall outside the confidence interval, e.g., five data points would be below a lower confidence interval. Examining Figures 1, 2 and 3, the total number of data points were 165, 390 and 165 respectively. It would be expected that 8, 20 and 8 data points would fall outside the confidence interval if it is truly a 95% confidence interval. In fact, only 6, 6 and 3 data points fall outside the confidence intervals. In the case of thermal expansion, a subset of the data was used for the regression and confidence interval. Even so, the upper 95% confidence interval encompasses all but a few data points from the complete data set. Based on these observations, the confidence intervals are in fact conservative for a 95% confidence interval and can be used for design purposes.

Specific Heat

The specific heat of a material can be calculated using a rule of mixtures type relationship (8). Using data from References 8 and 9, the specific heats of the average composition of Cu-6.62 wt.% Cr- 5.73 wt.% Nb were calculated from 0 K to 1358 K, the melting point of pure Cu. A comparison of the regression model and the rule of mixtures calculations is presented in Figure 9. With the exception of the highest temperatures, the regression values are within 1.5% of the calculated specific heat for the temperature range tested. At 1173 K, the difference was 3.25%.

Referring to Figure 2, the regression of the specific heat favors the higher values in the data at 1173 K. This error shows up as part of the lack of fit error term for the regression. Use of a higher order polynomial to fit the data would help to improve the agreement between the regression and calculated specific heat values at the highest temperatures. Even as is, the calculated values and the shape of the curve are very similar to the regression values. This helps to confirm the validity of the regression model.

Statistically significant variations between powder lots were observed at 296 K and above 623 K. In all cases powder lot 3C which has the greatest Cr+Nb content had the highest specific heat while powder lots 3B and 3D which have the lowest Cr+Nb contents were the lowest. Powder lots 3A and 3E had intermediate Cr+Nb contents and were generally not statistically different from the other powder lots. In those instances where there was a statistical difference, powder lot 3E, which has a slightly lower Cr+Nb content, was found to have a lower specific heat.

From this analysis, it can be seen that, even though the range of Cr+Nb contents is small (0.22 wt.%), the sensitivity of the test method made it possible to detect differences at certain temperatures. In practical terms, the variations in specific heat from the variations in Cr+Nb contents is small and is accounted for by using the values of the lower confidence interval in a design.

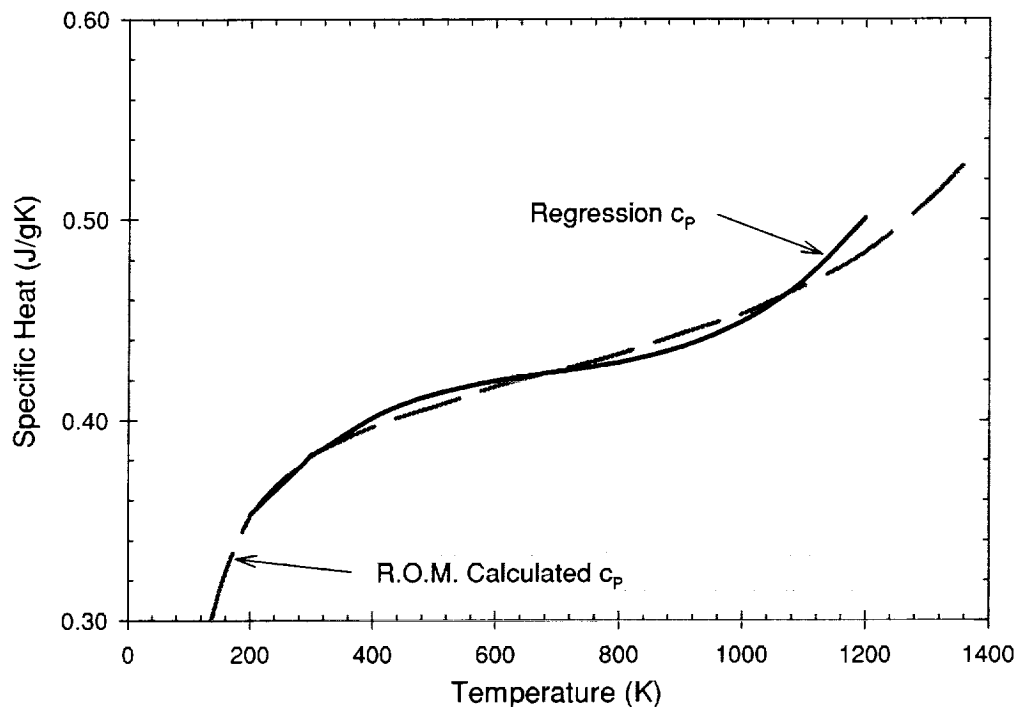


Figure 9 - Comparison of Regression and Calculated Specific Heat Values

Thermal Conductivity

In five cases, it was determined that there was a statistically significant difference in the thermal conductivity between powder lots. Referring back to the specific heat, most of the temperatures where the thermal conductivity is different correspond to the temperature range where differences were observed in the specific heats. From Equation 1, it is known that the thermal conductivity is proportional to the specific heat. It is therefore not surprising that the thermal conductivity shows lot-to-lot variations when the specific heat does. The same general rankings are observed as with the specific heat as well. Again, the sensitivity of the test method is sufficient to detect the small variations caused by the slight differences in chemistry. These differences are accounted for by using the lower confidence interval in a design.

The thermal conductivity of high purity Cu is 397 W/mK at room temperature (10). As shown in Figure 3, the thermal conductivity of GRCo-84 at room temperature is lower than pure Cu. However, it is still much higher than many materials with similar elevated temperature mechanical properties such as stainless steels (11).

The lower thermal conductivity relative to pure Cu is a concern since lowering the thermal conductivity increases the operating temperature. However, prior work (1-3) has shown GRCo-84 has significantly greater strength and maximum operating temperature capability. Using a yield strength of 100 MPa as the criteria for maximum operating temperature, GRCo-84 can be used up to 973 K while NARloy-Z is limited to 773 K. The lower thermal conductivity of GRCo-84 should translate into a much smaller temperature increase than 200 K. Therefore, the lower thermal conductivity should not preclude the use of GRCo-84 in thrust cell liners and many other applications.

In addition, the significantly higher strength of GRCo-84 can be used to redesign components. Since the strength of GRCo-84 is approximately twice that of NARloy-Z at 773 K, the cooling channel walls can be thinned while still maintaining a considerable safety margin. Therefore, while the lower thermal conductivity will increase the thermal gradient, thinning the walls may actually result in a lower hot wall temperature.

Currently the Rocketdyne Division of Boeing is conducting trade studies using the recently generated data to determine the effects of lowering the thermal conductivity. The chemical analysis of the extrusions shown in Table 1 also suggests another method to increase thermal conductivity through lowered impurity content.

Effect of Fe

The effect of Fe on the thermal conductivity cannot be directly determined at this point because the Fe contents of the five powder lots tested were very similar. However, using the effect of Fe on electrical resistivity as a guide, the relative effect of Fe on thermal conductivity may be assessed.

Pawlek and Reichel (12) reported a room temperature electrical resistivity of $1.68 \mu\Omega\cdot\text{cm}$ for pure Cu. The addition of 0.0150 wt.% Fe increases the electrical resistivity to $1.86 \mu\Omega\cdot\text{cm}$. Applying the Weidmann-Franz Law, this corresponds to a decrease in thermal conductivity of 11% or about 44 W/mK. In the GRCop-84 samples tested, the decreases in room temperature thermal conductivity relative to pure Cu average 115 W/mK. Therefore, the decrease from the Fe impurities alone could account for 38% of the total decrease in thermal conductivity.

This analysis does not take into account the possibility the Fe is present exclusively in the Cr_2Nb particles nor does it examine the possibility the Fe forms Fe-Cr precipitates. Both situations would not affect the thermal conductivity as severely as Fe being present in the Cu matrix. However, it does indicate the potential for a significant increase in thermal conductivity for the alloy. The economical viability of producing lower Fe content alloys may preclude its use for commercial applications, though.

Effect of Thermal Conductivity on Lorenz Number

The Lorenz number is generally referred to as a constant. However, Figure 6 clearly shows the value is dependent on temperature. Above approximately 120 K the Lorenz number slowly increases linearly with temperature. Below 120 K the Lorenz number rapidly increases. The deviation from a constant value can be traced to the changes in the thermal conductivity shown in Figure 4.

Between 120 K and 473 K, the thermal conductivity is slowly increasing in a near linear manner. The relative change is only slightly greater than that of the electrical resistivity. Consequently, the Lorenz number is increasing very slowly and could be considered constant. Below 120 K the thermal conductivity is rapidly increasing while the electrical resistivity continues to decrease linearly. Therefore, the Lorenz number rapidly increases.

The cause of the rapid increase in the thermal conductivity is related to the effects of imperfections such as dislocations and solute atoms on thermal conductivity. White (13) showed that pure Ag had two different dependencies of thermal conductivity on temperature based on the imperfections. A heavily deformed Ag sample showed no thermal conductivity maxima, but the same sample when annealed showed a maximum near 20 K. Above 20 K the thermal conductivity rapidly decreased and asymptotically approached a constant value above 50 K. The same basic behavior is observed in Figure 4 for GRCop-84. The differing behavior for Ag was attributed to the changing concentration of imperfections, in this case dislocations.

Matthiessen's Rule (14), which deals with the electrical resistivity of a metal, can be used to examine scattering of the electrons by static imperfections and phonons. In its general form, Matthiessen's Rule can be expressed as

$$\rho(T) = \rho_o + \rho_i(T) \quad [25]$$

where ρ_o is equal to the scattering from imperfections and $\rho_i(T)$ is the scattering from phonons. The scattering from imperfections is dependent on the concentration of imperfections but is independent of temperature. Figure 5 and Equation 19 indicate that GRCop-84 follows Matthiessen's Rule.

An analogous situation exists with the thermal resistivity (W). The thermal resistivity is given by the equation

$$W(T) = \frac{1}{\lambda(T)} = W_o(T) + W_i(T) \quad [26]$$

where $W_o(T)$ is the thermal resistivity from the imperfections and $W_i(T)$ is the thermal resistivity from the electron-phonon interactions.

Since the imperfections generally scatter the electrons elastically, the Wiedemann-Franz Law and the ideal value of the Lorenz number can be used to relate $W_o(T)$ to ρ_o . From this, it can be shown that the temperature dependency of $W_o(T)$ is proportional to $1/T$.

Since both W_o and W_i are dependent on temperature, the relative rates of change determine if there is a thermal conductivity maximum. If the value of W_o is near W_i at low temperatures, then the relative changes in the two values ($1/T$ versus T) results in a maximum in the thermal conductivity followed by a decrease to a limiting value. On the other hand, if a metal or alloy has a large imperfection concentration, then W_i and W_o become comparable only at high temperatures where W_o is already essentially constant. In this case, as shown by White, the thermal conductivity increases and asymptotically approaches the limiting value.

In the case of GRCop-84, the thermal conductivity will go through a maximum at some temperature below 50 K, probably near 30 K, the value for pure Cu (15). This indicates that the contribution from the imperfections to the thermal resistivity is low and comparable to the electron-phonon interactions only at very low temperatures. The

alloy was designed such that the matrix would be nearly pure Cu. From the analysis of the thermal conductivity and Lorenz number, it appears that this goal was achieved. It also indicates that the concentration of dislocations is low although the material was highly deformed during the extrusion process. From this it can be inferred that GRCo-84 is at least partially and probably fully recrystallized.

Low Temperature Electrical Resistivity

Only one specimen was tested to 29 K, so it is difficult to draw any definitive conclusions on the extremely low temperature electrical resistivity of GRCo-84. However, between 80 K and 150 K data exist from both data sets that can be compared. As shown in Figure 10, the TPRL and ORNL data have minimal overlap, but the regression lines are nearly parallel. If linear regression is conducted for just the data between 80 K and 150 K, the lines are parallel. The slight offset can probably be accounted for by laboratory to laboratory differences.

Consequently, the GRCo-84 electrical resistivity data can be extrapolated to 30 K using the data from ORNL as a guide. This allows comparison of the GRCo-84 electrical resistivity to other materials for applications such as high field strength magnets that will operate at these low temperatures. For comparison, the conductivity of pure Cu from Clark et al. (16) is also presented in Figure 10. In this temperature range, GRCo-84 has approximately half the electrical conductivity of pure Cu.

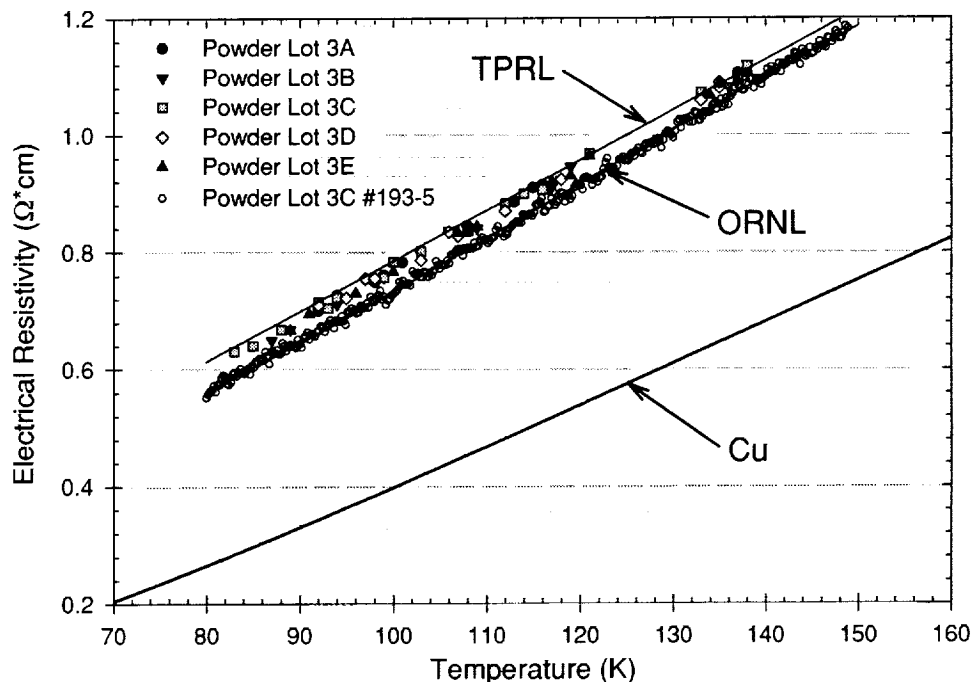


Figure 10 - Comparison of TPRL and ORNL Data Between 80 K and 150 K

Thermal Expansion

Thermally induced stresses are the primary stresses acting upon thrust cell liners. The hot wall side faces a flame near 3033 K (5000°F) while 1 mm away cryogenic hydrogen flows through the cooling channels. Thermal gradients in service are anticipated to be 300 to 600 K/mm or higher. Failure on the SSME liner is through a complex combination of creep, low cycle fatigue (LCF) and thermal ratcheting. If the thermally induced stresses can be reduced, the life of the liner can be greatly increased.

Figure 11 compares the average thermal expansion of previously tested NARloy-Z to GRCo-84. At a temperature of 773 K, the thermal expansion of GRCo-84 is 7.6% less than NARloy-Z. If one assumes that the stresses in the liner are directly proportional to the thermal expansion, then the thermally induced stresses will be lowered by the same amount. GRCo-84 has significantly higher creep resistance than NARloy-Z (3) that will lead to design changes in an optimized design. However, if a fixed design based on a stress for NARloy-Z to last 15 hours at 773 K in creep is used as a guide, one can calculate the effects of the lower thermally induced stresses. Based on prior creep testing, NARloy-Z can withstand a creep stress of 76.8 MPa for 15 hours. If GRCo-84 is subjected to the same stress, it will last 402 hours. Reducing the stress by 7% due to lower thermal expansion extends the creep life of GRCo-84 to 632 hours, a further increase of 57% in the creep life. This also represents a total increase of 41X over the NARloy-Z design life of 15 hours.

The strain range the liner undergoes during LCF will also be decreased by the lower thermal expansion. Using prior data (3) from LCF testing and the thermal expansions of NARloy-Z and GRCop-84 at 811 K, the LCF lives can be calculated. NARloy-Z subjected to a strain range of 0.98%, the strain from thermal expansion at 811 K, would last 2425 cycles. Decreasing the strain range from 0.98% to 0.90% by decreasing the thermal expansion would increase the GRCop-84 LCF life from 3600 cycles to 4900 cycles, an increase in life of 35%. Overall, the substitution of GRCop-84 for NARloy-Z would result in a doubling of LCF life.

By the substitution of GRCop-84 with its lower thermal expansion for NARloy-Z, the lives of thrust cell liners can be significantly enhanced.

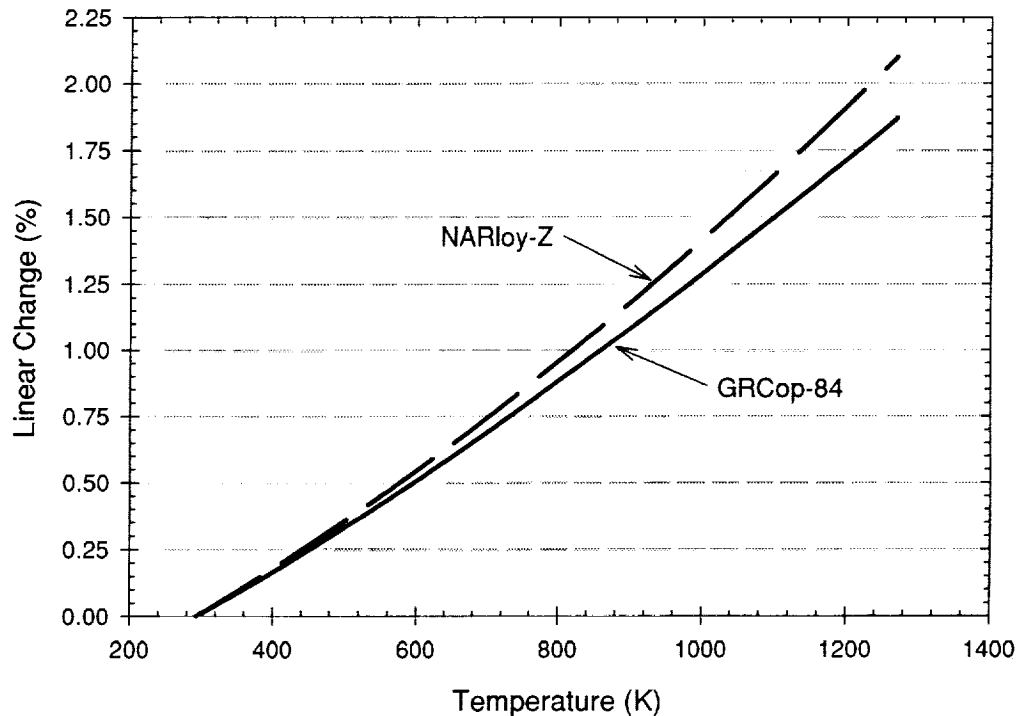


Figure 11 - Comparison of GRCop-84 and NARloy-Z Thermal Expansion

Summary and Conclusion

The thermal diffusivity, specific heat, thermal conductivity and thermal expansion of GRCop-84 were measured from cryogenic temperatures to at least 1173 K. In addition, the electrical resistivity was measured from 83 K to 475 K with one sample being measured down to 29 K. Three samples from each of five separate powder lots for fifteen samples were tested giving five true statistical repeats. The resulting data were analyzed using weighted regression to model the properties as a function of temperature and assign one-sided confidence intervals to the regressions.

Analysis and comparison to available thermophysical properties models showed that the regressions gave good agreement with the calculated values. These lend support to the statistical methods used for the regressions and confidence interval calculations.

The thermal conductivity of GRCop-84 was lower than Cu but still substantially better than many competitive materials with similar mechanical properties such as stainless steels. The lower thermal expansion of GRCop-84 compared to NARloy-Z may greatly increase the life of rocket engine liners.

Overall GRCop-84 is a viable alternative to Cu, NARloy-Z and other high conductivity materials for use in high temperature, high heat flux applications where good mechanical properties at temperature are required.

References

1. D.L. Ellis and R.L. Dreshfield, "Preliminary Evaluation of a Powder Metal Copper-8 Cr-4 Nb Alloy," Proc. of the Advanced Earth-to-Orbit Conference, NASA CP-3174, NASA MSFC, Huntsville, AL, (May 1992)
2. D.L. Ellis, R.L. Dreshfield, M.J. Verrilli, and D.G. Ulmer, "Mechanical Properties of a Cu-8 Cr-4 Nb Alloy," Earth-to-Orbit Conference, NASA CP-3282, NASA MSFC, Huntsville, AL (May 1994)
3. D.L. Ellis and G.M. Michal, *Mechanical and Thermal Properties of Two Cu-Cr-Nb Alloys and NARloy-Z*, NASA CR 198529, NASA Lewis Research Center, Cleveland, OH, (Oct. 1996)
4. M.A. Buckman, L.D. Bentsen, J. Makosey, G.R. Angell and D.P.H. Hasselman, *Trans. Brit. Cer. Soc.*, Vol. 82, No. 1, (1983), pp.18-23
5. P.G. Klemens, *Thermal Conductivity, Vol. 1*, ed. R.P. Tye, Academic Press, London and New York, 1969, p. 37.
6. *Transport Phenomena in Metallurgy*, G.H. Geiger and D.R. Poirier, Addison-Wesley Publ. Co., Reading, MA, (1973), p. 191
7. F. Bloch, *Z. Physik*, Vol. 59, (1930), p. 208
8. R.R. Hultgreen, *Selected Values of Thermodynamic Properties of the Elements*, ASM International, Metals Park, OH (1973)
9. *NIST-JANAF Thermochemical Tables, Fourth Ed., Part II, Cr-Zr*, M.W. Chase, Jr. Ed., American Institute of Physics for the National Institute of Standards and Technology, Washington, DC (1998)
10. *Smithells Metals Reference Book, 6th Ed.*, E.A. Brandes, Ed., Butterworths, London, (1983), p. 14-1
11. *Smithells Metals Reference Book, 6th Ed.*, E.A. Brandes, Ed., Butterworths, London, (1983), pp. 14-23 to 14-39
12. F. Pawlek and K. Reichel, "The Effect of Impurities On The Electrical Conductivity of Copper." *Zeit. Metallkunde*, Vol. 47, (1956), p. 347
13. G.K. White, *Proc. Phys. Soc. London*, Vol. A66, (1953), p. 844
14. A. Matthiessen and C. Vogt. *Ann. Phys. Leibz*, Vol. 122, (1964), p. 19
15. F.R. Schwartzberg, S.H. Osgood, R.O. Keys and T.F. Kiefer, *Cryogenic Materials Data Handbook*, The Martin Co., (Aug. 1964)
16. A.F. Clark, G.E. Childs and C.H. Wallace, "Low Temperature Electrical Resistivity of Some Engineering Alloys," *Cryogenic Materials Conference*, Univ. of California, (June 1969)

REPORT DOCUMENTATION PAGE

Form Approved
OMB No. 0704-0188

Public reporting burden for this collection of information is estimated to average 1 hour per response, including the time for reviewing instructions, searching existing data sources, gathering and maintaining the data needed, and completing and reviewing the collection of information. Send comments regarding this burden estimate or any other aspect of this collection of information, including suggestions for reducing this burden, to Washington Headquarters Services, Directorate for Information Operations and Reports, 1215 Jefferson Davis Highway, Suite 1204, Arlington, VA 22202-4302, and to the Office of Management and Budget, Paperwork Reduction Project (0704-0188), Washington, DC 20503.

1. AGENCY USE ONLY (Leave blank)		2. REPORT DATE June 2000	3. REPORT TYPE AND DATES COVERED Final Contractor Report	
4. TITLE AND SUBTITLE Thermophysical Properties of GRCop-84			5. FUNDING NUMBERS WU-242-23-54-00 NAS3-463	
6. AUTHOR(S) David L. Ellis and Dennis J. Keller				
7. PERFORMING ORGANIZATION NAME(S) AND ADDRESS(ES) Case Western Reserve University White Building 10900 Euclid Avenue Cleveland, Ohio 44106-7204			8. PERFORMING ORGANIZATION REPORT NUMBER E-12257	
9. SPONSORING/MONITORING AGENCY NAME(S) AND ADDRESS(ES) National Aeronautics and Space Administration John H. Glenn Research Center at Lewis Field Cleveland, Ohio 44135-3191			10. SPONSORING/MONITORING AGENCY REPORT NUMBER NASA CR-2000-210055	
11. SUPPLEMENTARY NOTES David L. Ellis, Case Western Reserve University, White Building, 10900 Euclid Avenue, Cleveland, Ohio 44106-7204; and Dennis J. Keller, RealWorld Quality Systems, Inc., 20388 Bonnie Bank Blvd., Cleveland, Ohio 44116. Project Manager, Michael Nathal, Materials Division, NASA Glenn Research Center, organization code 5120, (216) 433-9516.				
12a. DISTRIBUTION/AVAILABILITY STATEMENT Unclassified - Unlimited Subject Category: 26 This publication is available from the NASA Center for AeroSpace Information, (301) 621-0390.			12b. DISTRIBUTION CODE Distribution: Nonstandard	
13. ABSTRACT (Maximum 200 words) The thermophysical properties and electrical resistivity of GRCop-84 (Cu - 8 at.% Cr-4 at.% Nb) were measured from cryogenic temperatures to near its melting point. The data were analyzed using weighted regression to determine the properties as a function of temperature and assign appropriate confidence intervals. The results showed that the thermal expansion of GRCop-84 was significantly lower than NARloy-Z (Cu-3 wt.% Ag-0.5 wt.% Zr), the currently used thrust cell liner material. The lower thermal expansion is expected to translate into lower thermally induced stresses and increases in thrust cell liner lives between 2X and 41X over NARloy-Z. The somewhat lower thermal conductivity of GRCop-84 can be offset by redesigning the liners to utilize its much greater mechanical properties. Optimized designs are not expected to suffer from the lower thermal conductivity. Electrical resistivity data, while not central to the primary application, show that GRCop-84 has potential for applications where a combination of good electrical conductivity and strength is required.				
14. SUBJECT TERMS Thermal conductivity; Electrical resistivity; Specific heat; Thermal diffusivity; Cu alloys			15. NUMBER OF PAGES 23	
			16. PRICE CODE A03	
17. SECURITY CLASSIFICATION OF REPORT Unclassified	18. SECURITY CLASSIFICATION OF THIS PAGE Unclassified	19. SECURITY CLASSIFICATION OF ABSTRACT Unclassified	20. LIMITATION OF ABSTRACT	